Scaling fixed-field alternating-gradient accelerators with reverse bend and spiral edge angle

Shinji Machida

Published version information:

Citation: S Machida. "Scaling fixed-field alternating-gradient accelerators with reverse bend and spiral edge angle." Physical Review Letters, vol. 119, no. 6 (2017): 064802.

doi: 10.1103/PhysRevLett.119.064802

Scaling Fixed-Field Alternating-Gradient Accelerators with Reverse Bend and Spiral Edge Angle

Shinji Machida*
STFC Rutherford Appleton Laboratory, Harwell Campus, Didcot OX11 0QX, United Kingdom
(Received 25 January 2017; published 10 August 2017)

A novel scaling type of fixed-field alternating-gradient (FFAG) accelerator is proposed that solves the major problems of conventional scaling FFAGs. This scaling FFAG accelerator combines reverse bending magnets of the radial sector type and a spiral edge angle of the spiral sector type to ensure sufficient vertical focusing without relying on extreme values of either parameter. This new concept makes it possible to design a scaling FFAG for high energy (above GeV range) applications such as a proton driver for a spallation neutron source and an accelerator driven subcritical reactor.

DOI: 10.1103/PhysRevLett.119.064802

Particle accelerators were developed initially as a tool to explore particle physics at the energy frontier. Recently, however, many accelerators have been constructed for other fields of physics mostly with the aim of producing secondary or tertiary particles such as neutrons, muons, and neutrinos. Important in this area is the number of energetic particles, usually protons, that are used to create secondary or tertiary particles through impact with a production target. The energy of each particle does not have to be as high as in accelerators for research at the energy frontier; instead emphasis is put on the beam intensity, which is always demanding. The research field that this type of accelerator explores is called the intensity frontier, and the accelerator is usually referred to as a proton driver.

Considering the cross section of the secondary and tertiary particle production, the energy of a proton driver covers a range from a few 100 MeV to some 10's of GeV. Cyclotrons cover the lower end: the machines at PSI and TRIUMF, for example, have just enough energy for neutron and muon production. Linear accelerators (linacs for short) with and without an accumulator ring and rapid cycling synchrotrons (RCS) usually produce beams of a few GeV to produce neutrons most efficiently. ISIS, SNS, J-Parc RCS, and ESS (under construction in Sweden) belong to this category. When protons with energies higher than a few GeV are required for the production of kaons and neutrinos through pions, slow cycling synchrotrons are the only option. BNL-AGS, CERN-PS, and J-Parc MR are examples.

Fixed-field alternating-gradient (FFAG) accelerators were invented in the 1950s and developed over the following years, initially as accelerators for energy frontier physics [1,2]. At the same time, an alternating-gradient synchrotron had been developed and its more compact magnets relative to the FFAGs became a big advantage when looking to increase beam energy, so the objectives of the FFAG accelerator development faded out. Although there remained pockets of interests on FFAG accelerators, for instance [3–7], little development beyond paper studies took place until the late 1990s when the idea of a neutrino factory called for an accelerator that could rapidly accelerate muons before they had time to decay [8–10].

When FFAGs were invented, it was realized that an important advantage over other types of accelerators was their potential for high beam intensity with an energy range covering a few GeV. Although cw operation of cyclotrons is the simplest way to obtain high average beam intensity, the energy range is limited below ~1 GeV. At higher energies, the size of cyclotrons becomes too large and also beam extraction becomes difficult because the turn separation at the outer orbits is minimal. Although the fixed field nature of FFAGs requires relatively large magnets to cover the orbit excursion from injection to extraction energy, the magnetic fixed field nature also enables rapid acceleration as well as a high repetition rate of operation as long as the rf acceleration system can provide sufficient power. This is opposite to the synchrotron limitation due to existing limits on magnet field variations.

In the last 15 years, there has been significant progress in the development of FFAG accelerators. For high intensity applications, a proof of principle model with 1 MeV output energy was constructed at KEK [11]. Two scaled-up machines, one a prototype for medical applications [12] and the other for a proton driver to drive an accelerator driven subcritical reactor (ADSR) [13] were constructed at KEK and Kyoto University, respectively.

Both machines follow the scaling FFAG design and have a vertical magnetic field profile given by

$$B_z(r,\theta) = B_{z0}\left(\frac{r}{r_0}\right)^k F(\varphi), \tag{1}$$

where

$$\varphi = \theta - \tan\delta \ln\frac{r}{r_0}$$

is the generalized azimuthal angle, r is the radial coordinate, θ is the geometrical azimuthal angle, r_0 and B_{z0} are

the reference radius and the vertical magnetic field at the reference radius, respectively, as shown in Fig. 1, and k is the geometrical field index defined as

$$k = \frac{r}{B_z}\left(\frac{\partial B_z}{\partial r}\right).$$

$F(\varphi)$ is a periodic function with period $2\pi/N$, where N is the number of cells in the ring. δ is the spiral edge angle.

With this magnetic field profile, the scaling FFAG satisfies the scaling conditions,

$$\frac{\partial}{\partial p}\left(\frac{K}{K_0}\right)\bigg|_{\varphi=\text{const}} = 0, \tag{2}$$

$$\frac{\partial k}{\partial p}\bigg|_{\varphi=\text{const}} = 0, \tag{3}$$

where K is the local curvature of the orbits and K_0 refers to the average curvature defined by 2π/(the orbit length); p is the beam momentum. Equation (2) indicates the orbits with different momenta have geometrical similarity and Eq. (3) indicates the geometrical field index k is constant at corresponding orbit points. The scaling conditions make the transverse tune of strong focusing accelerators constant with fixed field magnets and avoid resonance crossing during acceleration. For extremely fast acceleration for short lived particles like muons, however, this can be violated, which leads to the concept of a nonscaling FFAG [14]. Very fast acceleration without the scaling condition was first demonstrated in the electron model for many applications (EMMA) project in the United Kingdom in 2012 [15].

In practice, scaling FFAGs are realized by two different types of structure. One is based on radial sector magnets [16] and the other uses a spiral sector structure [17] and depends on the form of $F(\varphi)$ in Eq. (1). A radial sector FFAG employs the function $F(\varphi)$ to flip the sign periodically so that normal and reverse bending magnets provide alternating focusing. In a spiral sector FFAG, the function $F(\varphi)$ is always positive with only normal bending magnets, but the magnet pole face has a finite edge angle with respect to the orbits, which gives the lattice magnets a spiral shape when viewed from above. The proper edge angle introduces a strong defocusing in the horizontal direction as opposed to the focusing in the body field of the magnets. Both the radial and spiral sector FFAGs that were constructed in the 1950s accelerated electrons to a few 100 keV. Recently a spiral FFAG for proton acceleration up to 2.5 MeV and two radial FFAGs up to 150 MeV were constructed in Japan [13].

FFAGs face practical problems to reach energies beyond a GeV to be competitive with linacs and synchrotrons. The number of cells has to increase to keep the individual magnets within reasonable field strengths and lengths. As a result, the bending angle per cell becomes relatively small. Either the spiral angle should be large or the strength of the reverse bending magnets should be high to keep enough vertical focusing. For example, when the strength of normal and reverse bends are equal, the reverse bend magnet can be made no shorter than about 2/3 of the normal bend to preserve vertical stability. The circumference of the machine is five times that which would be necessary if there were no reverse bend magnet [1]. This problem was not seen in the prototype FFAGs which do not have as many cells because of their lower energies [18].

This paper proposes a novel scaling FFAG that solves the difficulties by combining the principles of radial and spiral FFAGs. It is referred to as *DF-spiral FFAG* because spiral shaped defocusing and focusing magnets characterize the lattice. It can be regarded as either a small spiral angle added to a radial FFAG or a small reverse bend added to a spiral FFAG.

In scaling FFAGs, the ring tunes $Q_{x,z}$ are approximated by the following equations, (4) and (5), as long as $Q_{x,z}^2 \ll (N/2)^2$ [2], as

$$Q_x^2 \approx 1 + k + \frac{k^2 S^2}{N^2 b_0^2}, \tag{4}$$

$$Q_z^2 \approx -k + \frac{k^2 S^2}{N^2 b_0^2} + \frac{\Phi^2}{b_0^2}(1 + 2\tan^2\delta), \tag{5}$$

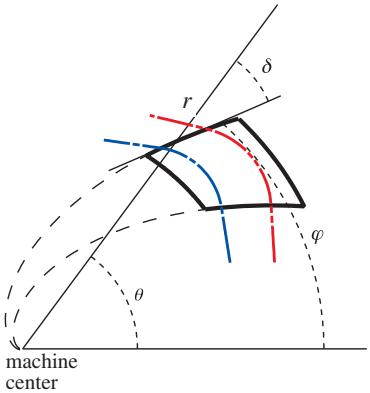

FIG. 1. Schematic diagram showing geometrical configuration of a FFAG magnet defined by Eq. (1). Orbit with low momentum (line with one dot, blue color) and orbit with high momentum (line with two dots, red color) have geometrical similarity as indicated by Eq. (2).

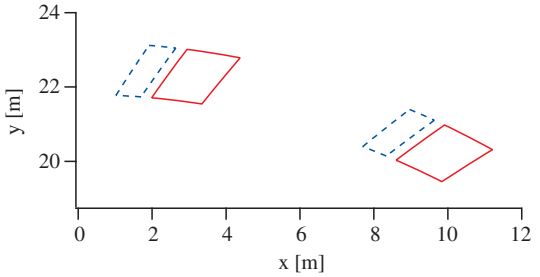

FIG. 2. Top view of DF-spiral FFAG lattice. The red solid line indicates a normal bending magnet and the blue dashed line identifies a magnet with reverse bend. Coordinates (0,0) give the machine center and the orbit radius is about 23 m. The spiral angle is 30° in this example. Refer to Table I for other parameters.

where the $\{b_m\}$ are defined as Fourier expansion coefficients for the vertical field in the azimuthal direction:

$$B_z = B_{z0} \sum_{m=0}^{\infty} b_m e^{imN\theta}$$

and

$$\Phi^2 = 4 \sum_{m=1}^{\infty} |b_m|^2,$$

$$S^2 = 2 \sum_{m=1}^{\infty} \frac{|b_m|^2}{m^2},$$

where N is the total number of cells in the ring lattice. The quantity Φ/b_0 is called the field flutter. The term $2\Phi^2 \tan^2 \delta / b_0^2$ is a measure of the specific strong focusing due to the spiral field shape. In short, the vertical tune is a function of the field flutter Φ/b_0 and the spiral angle δ. In a radial sector FFAG, the spiral angle is zero and the tune is dominated by the field flutter. In a spiral sector FFAG, the tune is adjusted by the spiral angle because the field flutter is almost unity since there are only normal bending magnets.

It is clear that making both the field flutter and the spiral angle adjustable at the same time gives more flexibility and better optimization for the vertical focusing without relying on extreme values of either parameter. This can be realized, for instance, by placing normal and reverse bending magnets next to each other with a finite spiral angle to make a doublet focusing cell as shown in Fig. 2. As a result, the edge focusing is enhanced in the vertical direction as we show below.

In order to obtain a more quantitative estimate, consider a design of a 1.2 GeV proton machine as an example. It consists of 20 identical cells with a 3.6° normal bending magnet (Bf) and a 1.8° reverse bending magnet (Bd). The ratio of integrated Bd and Bf strengths, the spiral angle, and the geometrical field index are the three, free parameters that we explore. The nominal average radius is 23 m so the maximum field strength is within the reach (∼1.8 T) of normal conducting magnets. The long drift space is about 5 m, which is enough for the injection and extraction systems and rf cavities. The main parameters are listed in Table I.

The edges of the Bd and Bf magnets are curved with a nonzero spiral angle and the field falls off according to Enge function [19] [Eq. (7)]. To ensure the scaling conditions, the vertical magnetic field on the midplane of each magnet is modeled as a function of the azimuthal angle as

$$B_z(r,\theta,0) = B_{z0}\left(\frac{r}{r_0}\right)^k \times E(-\theta + \theta_{b1} + \tan\delta \ln(r/r_0), \Delta\theta_{f1}) \times E(\theta - \theta_{b2} - \tan\delta \ln(r/r_0), \Delta\theta_{f2}), \quad (6)$$

where Enge function $E(s,\Delta s)$ is defined as

$$E(s,\Delta s) = \frac{1}{1+\exp\left(\sum_{i=0}^{5} C_i \left(\frac{s}{\Delta s}\right)^i\right)}, \quad (7)$$

TABLE I. Main parameters of the test lattice.

Parameter	Value	Unit
Number of cell	20	-
Nominal radius	23	m
Effective length of Bd	1.8	degs
Fringe length of Bd	0.75 (Bf side)	degs
	1.5 (other end)	degs
Effective length of Bf	3.6	degs
Fringe length of Bf	0.75 (Bd side)	degs
	1.5 (other end)	degs
Short drift space between Bd and Bf Long drift space	0.75	degs
	10.35	degs
Enge coefficients C_i $(i = 0, 5)$	0.1455, 2.267, −0.6395, 1.1558, 0, 0	

where θ_{b1} and θ_{b2} are the azimuthal positions of the effective boundaries, $\Delta\theta_{f1}$ and $\Delta\theta_{f2}$ are the characteristic lengths of the fringe regions, and C_i is Enge coefficients. The magnetic fields in other directions (B_r and B_θ) as well as B_z off the midplane are derived from Maxwell's equations up to the fourth order in z.

Once the lattice magnets are specified, the multiparticle tracking code SCODE [20] is used to calculate the ring optics and the particle beam dynamics. The equilibrium orbits for different momenta are found iteratively. A one-turn (or one-cell) transfer map is constructed using several test particles with different initial conditions with small amplitudes in each coordinate. The betatron tunes and lattice functions are calculated based on this map.

The advantage of the DF-spiral configuration is illustrated in Fig. 3 where an optical study is made using the ratio of integrated Bd and Bf strength to represent the field flutter, as in Eq. (5), for varying spiral angle.

Figure. 3(a) shows the domain that gives stable betatron oscillations when the geometrical field index is $k = 17$. The contours correspond to vertical cell tunes from 0 to 0.5 (0° to 180° phase advance). It should be noted that in a conventional radial sector FFAG, the variable parameter is the Bd/Bf ratio and is allowed to move only on the y axis. When the phase advance per cell is around 90°, the Bd/Bf ratio has to be around 0.5. Normal bending angle is canceled by reverse bending to a half. Compared with the lattice without reverse bending, the machine circumference is three times as much. With DF-spiral design to obtain the same phase advance, the Bd/Bf ratio can be 0.23 as shown later, which makes the machine circumference only ∼60% larger. In a conventional spiral sector FFAG, on the other hand, the spiral angle is the variable parameter and so the variation is along the x axis. A spiral angle of about 60° is not entirely impractical, but the main lattice magnets becomes very complex. Now we have the whole 2D region in parameter-space which gives us moderate choices for the spiral angle and the flutter factor simultaneously.

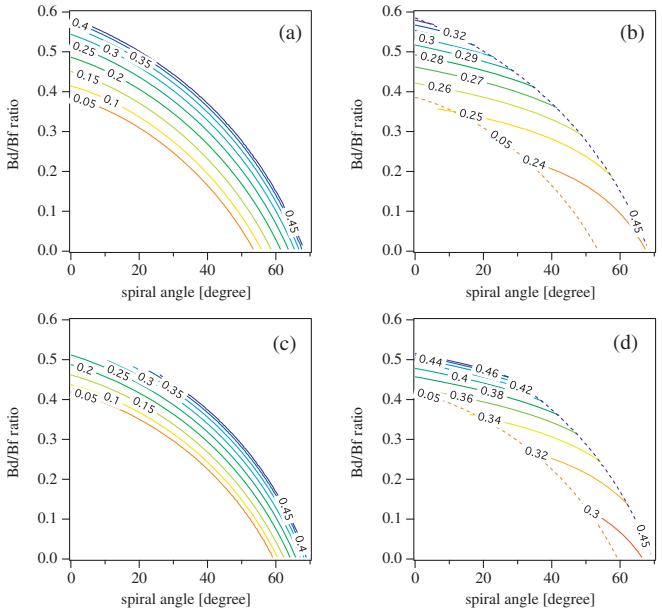

FIG. 3. Stable area with cell tune indicated as contour curve (a) with vertical cell tune when $k = 17$, (b) with horizontal cell tune when $k = 17$, (c) with vertical cell tune when $k = 25$, and (d) with horizontal cell tune when $k = 25$.

Figure 3(b) shows the same stable regions for varying horizontal cell tune. The horizontal cell tune is less sensitive to the parameters although it is clear that the higher Bd/Bf ratio leads to higher horizontal tune. The whole stable area is determined by the vertical stability.

With larger value of k, e.g. $k = 25$, which decreases the orbit excursion inversely proportional to k according to Eq. (1), the stable area shrinks as shown in Fig. 3(c). The variation of horizontal cell tune becomes larger within the stable area as shown in Fig. 3(d). The whole stable area is still mainly determined by the vertical cell tune, but in the region of high Bd/Bf, the horizontal cell tune reaches 0.5 and sets the stability boundary.

One of the major concerns of FFAG accelerators is dynamic aperture, which may become deteriorated by intrinsic nonlinearities of the lattice magnets [21]. The DF-spiral concept is not an exception. Two different constraints are imposed in order to explore dynamic aperture in the tune space. The first fixes the spiral angle at 30° and adjusts the Bd/Bf ratio together with k. The other fixes the Bd/Bf ratio at 0.23 and adjusts the spiral angle together with k. We label the former "DF-spiral A" and the latter "DF-spiral B".

The absolute strength of the magnets was adjusted to make the average orbit around 23 m for 1.2 GeV proton beams. The dynamic aperture is defined as the initial horizontal amplitude with which a particle can survive for 5000 turns at a fixed energy of 0.4 GeV, which is the nominal injection energy of the 1.2 GeV FFAG accelerator. The 5000 turns corresponds to a time scale of 5 ms in this size accelerator. Synchrotron oscillations are ignored. The initial vertical amplitude was fixed at 100 π, mm mrad.

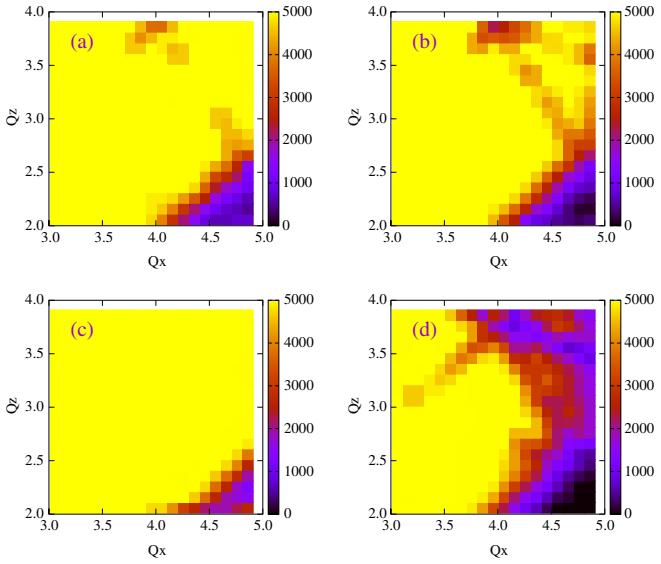

FIG. 4. Dynamic aperture of lattice configurations (a) DF-spiral A, (b) DF-spiral B, (c) radial sector, and (d) spiral sector in ring tune space $Q_x = 3.0$ to 5.0 and $Q_z = 2.0$ to 4.0. Dynamic aperture is defined as the maximum initial horizontal amplitude leading to particle survival for 5000 turns. The initial vertical amplitude is 100 π mm mrad. The color scale refers to horizontal amplitude in units of πmm mrad. Some systematic resonances, e.g. $2Q_x - 2Q_y = 0$ and $3Q_x + 2Q_y = 20$, can be identified.

In both DF-spiral A and B, horizontal dynamic apertures of more than 5000 π mm mrad are achieved at a certain tune region as shown in Figs. 4(a) and 4(b), respectively. Note that 5000 π mm mrad is the maximum aperture we have explored and about 10 times more than the physical aperture of similar energy proton drivers under operation [22,23]. Figures 4(c) and 4(d) show dynamic aperture of a conventional radial FFAG and a spiral FFAG, respectively, for comparison. The size of tune space area with large dynamic aperture in DF-spiral design is between radial and spiral FFAGs, at least no worse than the conventional design. Details of magnetic field distribution, especially in the fringe regions, is needed to evaluate more accurate dynamic aperture. It may be different from the simplified model we used due to magnet saturation and detail shape of magnet pole and coils. Calculation based on a 3D field map is one of the future study items.

In this paper, a novel scaling FFAG has been proposed which has features of both conventional radial and spiral sector FFAGs. The name *DF-spiral FFAG* is suggested. Having simultaneous vertical strong focusing from reverse bending magnets and spiral edge focusing eases the requirement from each function and provides increased confidence that such a design is achievable.

A 1.2 GeV proton FFAG design with a 20 cell lattice has been used as an example. The important property of dynamic

aperture has been calculated and shows no reduction in aperture compared with conventional radial and spiral sector FFAGs. The study demonstrates that there are indeed advantages in the DF-spiral design, which could well play a part in the development of future fixed field accelerators.

We wish to acknowledge the encouragement by Christopher Prior and support from members of the ISIS department at Science and Technology Facilities Council's Rutherford Appleton Laboratory.

*shinji.machida@stfc.ac.uk

[1] K. R. Symon, D. W. Kerst, L. W. Jones, L. J. Laslett, and K. M. Terwillinger, Fixed-field alternating-gradient particle accelerators, Phys. Rev. **103**, 1837 (1956).

[2] A. A. Kolomensky and A. N. Lebedev, *Theory of Cyclic Accelerators* (North-Holland, Amsterdam, 1966), p. 332.

[3] Y. Ishikawa *et al.*, in *Proceedings of the 8th meeting of the International Collaboration on Advanced Neutron Sources* (1985), p. 17, http://purl.org/net/epubs/work/42064.

[4] R. L. Kustom, T. K. Khoe, and E. A. Crosbie, A 1500-MeV fixed-field alternating-gradient synchrotron for a pulsed-spallation neutron source, IEEE Trans. Nucl. Sci. **32**, 2672 (1985).

[5] P. F. Meads, Jr. and G. Wüstefeld, An FFAG compressor and accelerator ring studied for the German spallation neutron source, IEEE Trans. Nucl. Sci. **32**, 2697 (1985).

[6] S. A. Martin, E. Zaplatin, P. F. Meads, Jr., G. Wüstefeld, and K. Ziegler, in *Proceedings of the 13th International Conference on Cyclotrons and their Applications, Vancouver, BC, Canada*, (JACoW, Vancouver 1992), p. 701, http://accelconf.web.cern.ch/AccelConf/c92/papers/xii-02.pdf.

[7] H. Jungwirth, R. L. Kustom, S. Martin, P. F. Meads, Jr., E. Zaplatine, and K. Ziegler, in *Proceedings of the 14th International Conference on Cyclotron and their Applications*, (JACoW, Cape Town 1995), p. 625, http://accelconf.web.cern.ch/AccelConf/c95/papers/l-08.pdf.

[8] F. Mills, in *Fourth International Conference Physics Potential, Development of* $\mu^+\mu^-$ *Colliders, 1997*, Transparency Book (University of California Los Angeles, unpublished), pp. 693–696.

[9] C. Johnstone, in *Fourth International Conference Physics Potential, Development of* $\mu^+\mu^-$ *Colliders, 1997*, Transparency Book (University of California Los Angeles, unpublished), pp. 696–698.

[10] S. Machida, Neutrino Factory design based on FFAG, Nucl. Instrum. Methods Phys. Res., Sect. A **503**, 41 (2003).

[11] M. Aiba, K. Koba, S. Machida, Y. Mori, R. Muramatsu, C. Ohmori, I. Sakai, Y. Sato, A. Takagi, R. Ueno, T. Yokoi, M. Yoshimoto, and Y. Yuasa, in *Proceedings of European Particle Accelerator Conference 2000* (JACoW, 2000), p. 581, http://accelconf.web.cern.ch/AccelConf/e00/PAPERS/MOP1B21.pdf.

[12] T. Adachi, M. Aiba, K. Koba, S. Machida, Y. Mori, A. Mutoh, J. Nakano, C. Ohmori, I. Sakai, Y. Sato, M. Sugaya, A. Takagi, R. Ueno, T. Uesugi, T. Yokoi, M. Yoshii, M. Yoshimoto, and Y. Yuasa, in *Proceedings of Particle Accelerator Conference 2001* (JACoW, 2001), p. 3254, http://accelconf.web.cern.ch/AccelConf/p01/PAPERS/RPPH016.PDF.

[13] M. Tanigaki, Y. Mori, M. Inoue, K. Mishima, S. Shiyoya, Y. Ishi, S. Fukumoto, and S. Machida, in *Proceedings. of European Particle Accelerator Conference 2006* (JACoW, 2006), p. 2367, http://accelconf.web.cern.ch/AccelConf/e06/PAPERS/WEPCH186.PDF.

[14] C. Johnstone, W. Wan, and A. Garren, in *Proceedings of the 1999 Particle Accelerator Conference, New York, 1999* (JACoW, 1999), p. 3068, http://accelconf.web.cern.ch/AccelConf/p99/PAPERS/THP50.PDF.

[15] S. Machida *et al.*, Acceleration in the linear non-scaling fixed-field alternating-gradient accelerator EMMA, Nat. Phys. **8**, 243 (2012).

[16] F. T. Cole, R. O. Haxby, L. W. Jones, C. H. Pruett, and K. M. Terwilliger, Electron model fixed field alternating gradient accelerator, Rev. Sci. Instrum. **28**, 403 (1957).

[17] D. W. Kerst, E. A. Day, H. J. Hausman, R. O. Haxby, L. J. Laslett, F. E. Mills, T. Ohkawa, F. L. Peterson, E. M. Rowe, A. M. Sessler, J. N. Synder, and W. A. Wallenmeyer, Electron model of a spiral sector accelerator, Rev. Sci. Instrum. **31**, 1076 (1960).

[18] The orbit excursion and therefore the radial width of the magnets does not much depend on the beam energy. From Eq. (1), the orbit excursion is roughly proportional to r_0/k with fixed momentum ratio from injection to extraction. The total number of cells N is proportional to, say $\sqrt{p}$, and $k \propto N^2$ from later Eqs. (4) and (5), r_0/k is a weak function of p.

[19] H. A. Enge, *Focusing of Charged Particles*, edited by A. Spetier (Academic Press, New York, 1967), Vol. 2, p. 203.

[20] S. Machida, S-code for fixed field alternating gradient accelerator design and particle tracking, Int. J. Mod. Phys. A **26**, 1794 (2011)

[21] M. Yoshimoto, T. Adachi, M. Aiba, S. Machida, Y. Mori, A. Muto, R. Muramatsu, C. Ohmori, I. Sakai, M. Sugaya, A. Takagi, R. Ueno, A. Yamazaki, T. Yokoi, Y. Yonemura, M. Yoshii, Y. Yuasa, and K. Koba, in *Proceedings of European Particle Accelerator Conference 2002* (JACoW, 2002), p. 1320, http://accelconf.web.cern.ch/AccelConf/e02/PAPERS/WEPLE062.pdf.

[22] S. M. Cousineau, in *Proceedings of HB2016, Malmö* (2016), p. 9, http://accelconf.web.cern.ch/AccelConf/hb2016/papers/moam4p40.pdf.

[23] H. Hotchi, H. Harada, S. Kato, M. Kinsho, K. Okabe, P. K. Saha, Y. Shobuda, F. Tamura, N. Tani, Y. Watanabe, K. Yamamoto, M. Yamamoto, and M. Yoshimoto, in *Proceedings of HB2016*, Malmö (2016), p. 480, http://accelconf.web.cern.ch/AccelConf/hb2016/papers/tham6x01.pdf.